Exploring Sum Rate Maximization in UAV-based Multi-IRS Networks: IRS Association, UAV Altitude, and Phase Shift Design

Yabo Li, Haijun Zhang, *Senior Member, IEEE*, Keping Long, *Senior Member, IEEE*, and Arumugam Nallanathan, *Fellow, IEEE*

***Abstract*—This paper studies the unmanned aerial vehicle (UAV) based multiple intelligent reflecting surface (IRS) network, where the hovering UAV acts as a base station, and the IRS enhances signal transmission to across obstacle between users and UAV. To achieve the maximum sum rate of proposed communication scenario, a non-convex problem considering IRS association results, hovering altitude of UAV, and the phase shift design of multi-IRS is formulated. From the IRS association problem, we can find that the IRS association results are coupled to the decoding order of non-orthogonal multiple access (NOMA). To tackle this, a mathematical interference expansion scheme is developed to decouple it and transform it to convex by binary relaxation method. The non-convexity of hovering altitude optimization problem is solved by logarithm operation, approximation, and auxiliary matrices. For the phase shift optimization problem of multi-IRS, we propose a gradient approximation based initial scheme and develop a univariate optimization based approach on the basis to achieve the users sum rate improvement in multi-IRS. In the end, we compare the proposed scheme with baseline scheme to present the superiority of this work under various network settings. The internal reasons for the variation of simulation results are also analyzed.**

***Index Terms*—Multi-IRS, sum rate maximization, UAV, IRS association, hovering altitude, phase shift.**

I. Introduction

The intelligent reflecting surface (IRS) has been selected as a potential communication medium that can improve the radio propagation environment intelligently in recent years [1]–[5]. IRS is composed of a set of intelligent reflecting elements, and every reflecting element could improve the quality of the initial received signal singly, generally including: phase, frequency, and amplitude [6]. The current research on IRS mainly considers the phase shift for performance improvement of the transmit signal, so the IRS needs no extra transmission power, which is energy efficient and different from other technologies. As for the IRS deployment, it is usually fixed on the outward wall of mansions, mobile vehicles, and ceilings to help the information transmission for transmitters and receivers in the base station (BS) scenarios. Additionally, the integrated utilization of IRS and other network technologies can give full play to its effectiveness, such as unmanned aerial vehicle (UAV) [7], non-orthogonal multiple access (NOMA) technology [8], multiple-input and multiple-output [9], [10], etc.

Y. Li, H. Zhang, and K. Long are with the Beijing Engineering and Technology Research Center for Convergence Networks and Ubiquitous Services, University of Science and Technology Beijing, Beijing 100083, China (e-mail: liyabo@xs.ustb.edu.cn; haijunzhang@ieee.org; longkeping@ustb.edu.cn).

A. Nallanathan is with the School of Electronic Engineering and Computer Science, Queen Mary University of London, London E1 4NS, U.K. (e-mail: a.nallanathan@qmul.ac.uk).

A. Related Works and Motivation

Initially, the researchers proposed to deploy a single IRS to improve the wireless propagation environment in special areas. For example, in [11], the authors designed a single-IRS based multi-user network, where the problem of active BS precoding and IRS reflecting coefficient for the goal of minimum mean square error was solved. In [12], the authors investigated the deployment scenarios both in indoor and outdoor environment, and revealed the performance gain improved by deployed IRS. In [13], the IRS was integrated to the study of multi-direction beamforming, and the authors proposed a successive signal detection method to optimize the data amount yielded from systems. In [14], the authors focused on the tradeoff between network capacity and consumed power by users in IRS networks, where the reflecting units in IRS was solved and added into the joint optimization design. The performance of self-sustainable IRS was studied and unveiled in [15]. In [16], the authors combined the index modulation with IRS networks and proposed a spatial modulation scheme for data rate optimization. In [17], a single IRS was designed to enhance the communication of ultra-reliable and low-latency based industrial automation with energy harvesting. While in [18], the IRS was specially deployed on a UAV. The authors of it studied the UAV height and the number of elements optimization problem with mobile IRS. Also in the UAV based scenario, the authors in [19] studied the composite channel gain problem considering the wave interference under Rician fading environment. The proximal policy optimization was investigated to solve the beamforming design in [20] with ergodic constraints. Similarly, the same question was studied by [21], where the work focused on the ratio of data bits to capacity with the given setting bound in the absence of direct network link. The IRS was used to enhance the transmission at the common edge of two cellular BSs in [22], where the formulated problem considered the optimization of both resource and phase shift limited to the required service.

However, the research of single IRS cannot achieve the ultimate performance of the network. The development of multi-IRS deserves more attention for the large-capacity requirements of the future network. In [23], the authors studied the coverage probability in the double-IRS based communication system and optimized the reflecting beamforming for the

maximum coverage probability. In [24], the authors studied the statistical characterization and network model in multi-IRS networks, where two purpose oriented solutions were developed to show the ergodic network capacity and outage probability performance. In [25], the authors designed a multi-IRS network model to serve remote users, while the nearby users still communicated directly through the BS. The same design about remote and nearby users of BS can also be found in the [26], but the authors of this paper focused on NOMA design and highlighted the performance improvement brought by it based on the signal-to-interference-plus-noise (SINR) interfered by IRS. The degrees of freedom region based on IRSs was investigated in [27], where the authors revealed the influence mechanism of the elements number on the network. A cooperative multi-RIS based wireless network was studied in [28], where the closed-form expression of IRS reflecting coefficient optimization was given according to delay matching based method. However, the optimization for lots of elements can be burdensome for online transmission in IRS, so the authors in [29] studied the offline design and online optimization based scalable model. The physical layer security was introduced to IRSs in [30], where the authors designed a multi-IRS enhanced secure communication network. To maximize the capacity of line of sight (LoS) channel empowered multi-IRS network, the authors in [31] proposed a novel IRS beamforming solution. While in [32], the authors considered the statistical characterization of ground users for sum rate optimization. In [33], the authors studied the deterministic propagation model based signal behaviors and power scaling for IRSs. The authors also revealed that the performance of IRS network was improved faster, while the upper boundary was also limited. In [34], the authors constructed the weighted rate optimization model for total equipments considering unit modulus limits in the multi-IRS network and developed two valid schemes to design it.

Following the technological advancements of UAV networks [35], the combination of IRS and UAV is not too tough to achieve. This combination has also received a certain degree of attention because of the flexible communication. Generally, this combination is divided into airborne IRS scheme [18], [19], [36]–[38] and fixed IRS scheme [39]–[43]. In [18], the authors not only studied the problems previously discussed, but also divided the network into three settings with and without IRS to compare the efficacy in different settings. The optimal design in UAV-IRS setting was also displayed at last. In [19], the authors considered the wave interference of reflecting elements in airborne IRS, where the mathematical boundary for channel gain was derived through approximation assisted transformation of Gaussian distribution. In [36], the authors studied the phase error model with von Mises distribution and tried to use the designed model to present the air to air channel in mobile IRS networks. In [37], the authors simulated and analyzed the performance for UAV carried IRS systems, and the results presented the capacity improvement compared to the conventional UAV networks. In [38], the expected sum age-of-information was studied in UAV based IRS networks, where the altitude of UAV based IRS was optimized by proximal policy optimization based learning approach. In [39], the average achievable rate was maximized by the designed trajectory and beamforming solution. In [40], the reinforcement learning empowered trajectory design problem in the case of IRS enhanced UAV communications was researched, and the authors gave the reflecting coefficient optimization results through the iterative minimization method. In [41], the authors not only considered the trajectory optimization of the UAV, but also focused on the IRS scheduling problem. Moreover, the authors designed two different goals and schemes to present results. In [42], the authors developed a parametric approximation based successive convex approximation (SCA) method to complete the iterative design in IRS-assisted UAV model and revealed that the change of UAV trajectory was limited by IRS's size. The benefits of maneuvering of UAV to network performance were also highlighted in [42]. The secure UAV communication with IRS was considered in [43], where the authors proposed a three-stage process to protect signals to the legitimate user. In [44], the energy harvesting was considered in UAV based IRS networks with the power of sensitivity value, where two IRS empowered channel states were presented to select based on the selection possibility of it. In [45], the authors used the machine learning approach to handle the UAV movement and network beamforming in UAV based IRSs networks, where the utilization of IRS can significantly reduce the energy consumption of conventional UAV networks.

These researches presented models and mechanisms of UAV based IRS symbiotic wireless networks, but we can find that the authors focused on the problem of horizontal movement of UAV in the common context of IRS phase shift optimization. However, in some practical scenarios such as emergency rescue and other energy limited networks, the horizontal movement is often impractical because it consumes the limited energy of the UAV with the limited payload [46]. At the same time, the problem of studying the hovering altitude of UAV in line with the actual needs has not been studied under the setting of the fixed multi-IRS. Therefore, this work considers a hovering UAV based network that there are obstacles blocking communication to enrich the work of UAV-IRS. Based on this setting we utilize the multi-IRS to enhance the signal for guaranteeing the service of ground users. Besides, in order to improve downlink capacity and alleviate the scarcity of limited spectrum resources, we propose a NOMA-empowered IRS downlink design. Note that NOMA has been studied with IRS enhanced networks in [14], [45], but the performance of this combination in the UAV environment is still worthy of study. The effects of the channel environment, location deployment, and association of IRSs in UAV networks on the NOMA-empowered multi-IRSs are also an appealing study. Moreover, these researches mainly optimized the energy efficiency and minimum power consumption with a single IRS, the sum rate optimization in the network is still attractive for NOMA-empowered multi-IRS networks. Therefore, in this work we aim at maximizing the total sum rate of NOMA-empowered multi-IRS networks by solving the IRS association, hovering altitude of UAV, and phase shift design problems, while considering the coupling between IRS association results and successive interference cancellation (SIC) decoding order of

NOMA. During the solution to solve subproblems, the mathematical interference expansion, approximated transformation, and gradient approximation (GA) method are developed to reduce complexity.

B. Contributions

The following points are the main contributions:

- We first design a hovering UAV based multi-IRS network model considering the network characteristics of both IRS and UAV. Then, the problem is modeled as a non-convex optimization problem which maximizes sum rate of total NOMA empowered users with the limit of maximum association matrices, hovering altitude, and reflection angles of elements. To effectively settle this issue, we split it into a three-stage based optimization process, which consists of IRS association, hovering altitude of UAV, and phase shift design in multi-IRS networks.
- To solve the IRS association problem, the binary association coefficient is relaxed. An interference expansion scheme is developed to handle the decoupling of IRS association results and SIC decoding order of NOMA. Then, we use mathematical transformations and auxiliary matrices to resolve the non-convexity of the hovering deployment problem of the UAV. The phase shift design of multi-IRS is a typical multivariate optimization problem, and a univariate search scheme based on GA method is proposed to simplify the solving process.
- In the end, a three-stage joint optimization process is presented, and we discuss the complexity brought by the proposed solution. Numerical results indicates that the IRS association results obtained by relaxation and interference expansion scheme are binary, so the integer restoration is not required after the initial relaxation. At the same time, we compare the convergence of the algorithm under different conditions, as well as making comparisons among results generated by proposed algorithm and baseline scheme to verify the superiority of the work.

C. Paper Organization

The structure of this paper is divided into five main parts. In addition to the introduction and motivational elaboration in Section I above, Section II formulates the main problem of the paper. Section III describes the solving process of the formulated problem. Section IV lists and analyzes the simulation results. Section V summarizes the whole work.

II. System Model and Problem Formulation

A. System Model

The UAV-based multi-IRS networks are considered in Fig. 1, where users are served by the BS based UAV via coexisting IRS. The UAV is equipped with a single antenna, and the location can be denoted by

$$\mathbf{r} = [r_x, r_y, r_z]^T, \tag{1}$$

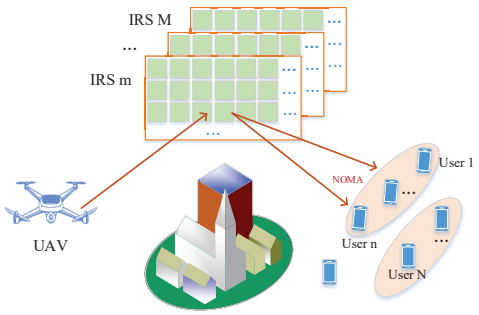

Fig. 1. Proposed UAV-based multi-IRS network with NOMA.

where the horizontal locations keep constant. The hovering altitude r_z is modeled to satisfy $r_z \in \left[r_z^{\min}, r_z^{\max}\right]$. $r_z^{\max}$ and $r_z^{\min}$ denote the extreme range of movement of hovering altitude that UAV can reach in this scene. The number of ground users is denoted by N, and the location of user n can be expressed as $\mathbf{u}_n = [u_n^x, u_n^y, 0]^T$. Considering the obstacles between ground users and the UAV, M IRSs are deployed at suitable locations to associate users. The channel state information (CSI) is set to be known by the network [39], [43]. The location of m-th IRS is denoted by

$$\mathbf{w}_m = [w_m^x, w_m^y, w_m^z]^T. \tag{2}$$

There are a total of K reflecting elements on each IRS, and the matrix of reflection coefficient of IRS m is denoted by

$$\mathbf{\Theta}_m = diag\left(e^{j\theta_{m,1}}, \cdots, e^{j\theta_{m,k}}, \cdots, e^{j\theta_{m,K}}\right), \tag{3}$$

where $\theta_{m,k}$ means the reflecting coefficient of k-th reflecting element on IRS m, and $\theta_{m,k} \in [0, 2\pi]$.

Let $\mathbf{g}_m \in \mathbb{C}^{K\times 1}$ represent the channel response vector between hovering UAV and IRS m. Assumed $\mathbf{g}_m$ utilize the Rician model [41] and can be denoted by

$$\mathbf{g}_m = \sqrt{\alpha_0 (d_m)^{-2}} \left(\sqrt{\frac{R_m}{R_m+1}} \mathbf{g}_m^{LoS} + \sqrt{\frac{1}{R_m+1}} \mathbf{g}_m^{NLoS} \right), \tag{4}$$

where α_0 represents the standard channel power when the propagation distance is 1m. d_m is the distance between the UAV and the IRS m, and it can be denoted by

$$d_m = \sqrt{\|\mathbf{r} - \mathbf{w}_m\|^2}, \tag{5}$$

R_m represents the Rician coefficient, and $\mathbf{g}_m^{NLoS}$ is the small scale fading which follows the complex Gaussian distribution with zero mean and variance 1. $\mathbf{g}_m^{LoS}$ is denoted by

$$\mathbf{g}_m^{LoS} = e^{-j\frac{2\pi d_m}{w}} \times \left[1, e^{-j\frac{2\pi d}{w}\cos\rho_m}, \cdots, e^{-j\frac{2\pi d(K-1)}{w}\cos\rho_m}\right], \tag{6}$$

where d and w denote the element spacing of IRS and wavelength of carrier, respectively. ρ_m denotes the angle of arrival (AoA). Similarly, let $\mathbf{g}_{m,n} \in \mathbb{C}^{K\times 1}$ represent the channel response vector between the IRS m and ground user n. $\mathbf{g}_{m,n} \in \mathbb{C}^{K\times 1}$ can be denoted by

$$\mathbf{g}_{m,n} = \sqrt{\alpha_0 (d_{m,n})^{-2}} \left(\sqrt{\frac{R_{m,n}}{R_{m,n}+1}} \mathbf{g}_{m,n}^{LoS} + \sqrt{\frac{1}{R_{m,n}+1}} \mathbf{g}_{m,n}^{NLoS} \right), \tag{7}$$

where $R_{m,n}$ represents the Rician coefficient, $\mathbf{g}_{m,n}^{NLoS}$ means the small scale fading which follows the same mathematical distribution as $\mathbf{g}_{m}^{NLoS}$. $\mathbf{g}_{m,n}^{LoS}$ is denoted by

$$\mathbf{g}_{m,n}^{LoS}=e^{-j\frac{2\pi d_{m,n}}{w}}\times\left[1,e^{-j\frac{2\pi d}{w}\cos\rho_{m,n}},\cdots,e^{-j\frac{2\pi d(K-1)}{w}\cos\rho_{m,n}}\right]. \tag{8}$$

Let $d_{m,n}$ and $\rho_{m,n}$ denote the distance and angle of departure, and we have

$$d_{m,n}=\sqrt{\|\mathbf{w}_m-\mathbf{u}_n\|^2}, and \tag{9}$$

$$\cos\rho_{m,n}=\frac{u_n^x-w_m^x}{d_{m,n}}. \tag{10}$$

Let $\mathbf{v}_{m,n}=\{\varpi_{m,n},\forall m,n\}$, where $\mathbf{v}_{m,n}$ denotes association matrix containing association coefficient $\varpi_{m,n}$, and $\varpi_{m,n}=1$ if IRS m is associated with user n, $\varpi_{m,n}=0$, otherwise. To stimulate the deployment effect of multi-IRS, we restrict the number of users that can be associated with the same IRS and can get

$$\sum_{n=1}^{N}\varpi_{m,n}\le\vartheta,\forall m. \tag{11}$$

Note that the existence of multi-IRSs provides a variety of options for users. It is more reasonable that the numerical size of ϑ should not be limited, because an IRS may fail to associate any users. That means that all users may be associated with the same IRS. Meanwhile, one user should be associated with one IRS, thus we can get

$$\sum_{m=1}^{M}\varpi_{m,n}=1,\forall n. \tag{12}$$

Specifically, each IRS uses the same subchannel, and NOMA is used to improve spectral efficiency from IRS to user. The SIC is employed at the user equipment to reduce interference by NOMA. Based on the decoding order from the channel condition, users which have the poorer channel state receive the interference from stronger one. Let $N_{m,n}$ denote the user set that can generate the interference to user n of IRS m obtained by the above channel condition based judgment rules, then the SINR and sum rate of ground user n served by IRS m is

$$SINR_{m,n}=\frac{p_{m,n}\left(\mathbf{g}_m^T\mathbf{\Theta}_m\mathbf{g}_{m,n}\right)^2}{\sum\limits_{n'\in N_{m,n}}p_{m,n'}\left(\mathbf{g}_m^T\mathbf{\Theta}_m\mathbf{g}_{m,n}\right)^2+\sigma^2}, and \tag{13}$$

$$\gamma_{m,n}=\varpi_{m,n}\log_2\left(1+\frac{p_{m,n}\left(\mathbf{g}_m^T\mathbf{\Theta}_m\mathbf{g}_{m,n}\right)^2}{\sum\limits_{n'\in N_{m,n}}p_{m,n'}\left(\mathbf{g}_m^T\mathbf{\Theta}_m\mathbf{g}_{m,n}\right)^2+\sigma^2}\right), \tag{14}$$

where $\sum\limits_{n'\in N_{m,n}}p_{m,n'}\left(\mathbf{g}_m^T\mathbf{\Theta}_m\mathbf{g}_{m,n}\right)^2$ represents the received interference from user n' by NOMA, $p_{m,n}$ and σ^2 denote the transmit power and noise power, respectively.

B. Problem Formulation

The goal of this work is to maximize the sum rate of the proposed UAV based multi-IRS NOMA network. Then the sum rate can be optimized by solving

$$\begin{aligned}&\max_{\mathbf{v}_{m,n},r_z,\mathbf{\Theta}_m}\sum_{m=1}^{M}\sum_{n=1}^{N}\gamma_{m,n}\\ s.t.\quad &C1:\varpi_{m,n}\in[0,1],\forall m,n,\\ &C2:\sum_{n=1}^{N}\varpi_{m,n}\le\vartheta,\forall m,\\ &C3:\sum_{m=1}^{M}\varpi_{m,n}=1,\forall n,\\ &C4:r_z\in\left[r_z^{\min},r_z^{\max}\right],\\ &C5:0\le\theta_{m,k}\le2\pi,\forall m,k.\end{aligned} \tag{15}$$

Problem (15) can be solved by optimizing IRS association matrix $\mathbf{v}_{m,n}$, UAV hovering altitude r_z, and IRS reflection matrix $\mathbf{\Theta}_m$. However, solving this problem directly has excessive complexity considering following some reasons. Firstly, the IRS association coefficient $\varpi_{m,n}$ is a binary variable and it determines the decoding order and interference to other users by NOMA in equation (14), which resulting in the coupling of IRS association and SIC decoding order. Second, the problem fundamentally shows non-convexity with respect to (w.r.t.) the UAV hovering altitude and reflecting coefficient matrices.

III. Multi-Stage Based Solution to Problem (15)

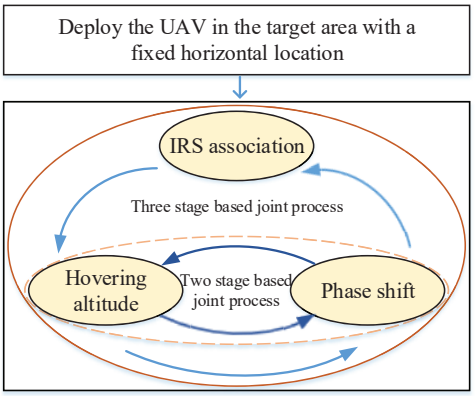

Fig. 2. The proposed multi-stage based optimization process.

In this section, problem (15) is divided into a three-stage based process to solve as shown in Fig. 2. First, the network will determine which user's signal will be enhanced by every IRS according to the IRS association results, when the UAV is deployed in a special scenario where the direct communication is difficult. Then, according to the assigned association results, we return to optimize the hovering altitude of UAV. Finally we optimize the design of multi-IRS utilizing the results-improved two solutions. Note that a two-stage based joint optimization process consisting of hovering altitude and phase shift is also developed to show the performance at last.

A. IRS Association

Substituting the known UAV altitude r_z and IRS reflection matrix $\mathbf{\Theta}_m$ into the equation (14), we can get the problem of the association matrix as follows:

$$\begin{aligned} &\max_{\mathbf{v}_{m,n}} \sum_{m=1}^{M}\sum_{n=1}^{N}\gamma_{m,n} \\ &s.t. \qquad C1-C3. \end{aligned} \tag{16}$$

$C1$ represents the binary of the association coefficient, $C2$ represents the maximum association number of users for an IRS, and $C3$ represents that each user should be associated and served by an IRS.
Restricted by the binary constraint $C1$, it is not effective to directly solve problem (16). Relaxing $\varpi_{m,n}$ as a continuous variable, and we can get

$$0 \le \varpi_{m,n} \le 1, \forall m, n. \tag{17}$$

Thus, the initial problem (16) can be converted to

$$\begin{aligned} &\max_{\mathbf{v}_{m,n}} \sum_{m=1}^{M}\sum_{n=1}^{N}\gamma_{m,n} \\ &s.t. \qquad C2, C3, (17). \end{aligned} \tag{18}$$

Note that IRS association results and SIC decoding order of NOMA are coupled, so the above problem cannot also be effectively solved considering the interference from NOMA to the co-IRS users. To efficiently handle it, an interference expansion scheme is developed below.

The original data rate of user n is $\gamma_{m,n}$ in equation (14), however let the user not be affected by the SIC decoding order when processing to the interference from NOMA, which means user with the poorest channel condition receives the interference from total users of all IRSs, we can rewrite $\gamma_{m,n}$ as

$$\gamma_{m,n}^{ex} = \varpi_{m,n}\log_2\left(1+\frac{p_{m,n}\left(\mathbf{g}_m^T\mathbf{\Theta}_m\mathbf{g}_{m,n}\right)^2}{\sum\limits_{n'\in N/n} p_{m,n'}\left(\mathbf{g}_m^T\mathbf{\Theta}_m\mathbf{g}_{m,n}\right)^2+\sigma^2}\right), \tag{19}$$

where we can see

$$\sum_{n'\in N/n} p_{m,n'}\left(\mathbf{g}_m^T\mathbf{\Theta}_m\mathbf{g}_{m,n}\right)^2 \ge \sum_{n'\in N_{m,n}} p_{m,n'}\left(\mathbf{g}_m^T\mathbf{\Theta}_m\mathbf{g}_{m,n}\right)^2, \tag{20}$$

and

$$\sum_{m=1}^{M}\sum_{n=1}^{N}\gamma_{m,n}^{ex} \le \sum_{m=1}^{M}\sum_{n=1}^{N}\gamma_{m,n}. \tag{21}$$

Therefore, the problem (18) can be represented by

$$\begin{aligned} &\max_{\mathbf{v}_{m,n}} \sum_{m=1}^{M}\sum_{n=1}^{N}\gamma_{m,n}^{ex} \\ &s.t. \qquad C2, C3, (17). \end{aligned} \tag{22}$$

Problem (22) is convex, and this paper uses CVX to solve it. Even if we scale the original problem in mathematical space, the optimal solution of the current (22) also satisfies problem (16) as a suboptimal solution. The detailed interference expansion scheme is shown in the following. Note that even though the IRS association coefficient $\varpi_{m,n}$ is relaxed to a continuous variable, the optimized results of (22) are still binary variables of 0 and 1, not a decimal. Therefore, there is no need to add another loop to the outer layer of algorithm 1 to improve the quality of the solution, iteratively.

Algorithm 1 Interference expansion scheme for IRS association

1: Initialize the hovering altitude r_z of UAV and IRS reflecting coefficient matrix $\mathbf{\Theta_m}$.
2: Get SIC decoding order based on the interference expansion scheme $\mathbf{v}_{m,n}^0$.
3: Get the IRS association matrix $\mathbf{v}_{m,n}$ via CVX by solving
$\max\limits_{\mathbf{v}_{m,n}} \sum\limits_{m=1}^{M}\sum\limits_{n=1}^{N}\left[\varpi_{m,n}\log_2\left(1+\frac{p_{m,n}\left(\mathbf{g}_m^T\mathbf{\Theta}_m\mathbf{g}_{m,n}\right)^2}{\sum\limits_{n'\in N/n} p_{m,n'}\left(\mathbf{g}_m^T\mathbf{\Theta}_m\mathbf{g}_{m,n}\right)^2+\sigma^2}\right)\right]$
$s.t. \quad C2, C3, (17).$
4: Update $\mathbf{v}_{m,n}$.
5: Update $\gamma_{m,n}$.

B. UAV Hovering Altitude

As for the hovering altitude of UAV, the problem (15) can be transformed to

$$\begin{aligned} &\max_{r_z} \sum_{m=1}^{M}\sum_{n=1}^{N}\gamma_{m,n} \\ &s.t. \qquad C4. \end{aligned} \tag{23}$$

To solve it, we can rewrite the objective as

$$\begin{aligned} \gamma_{m,n} &= \log_2\left(\sum_{n\in N_m} p_{m,n}\left(\mathbf{g}_m^T\mathbf{\Theta}_m\mathbf{g}_{m,n}\right)^2+\sigma^2\right) \\ &\quad -\log_2\left(\sum_{n'\in N_{m,n}} p_{m,n'}\left(\mathbf{g}_m^T\mathbf{\Theta}_m\mathbf{g}_{m,n}\right)^2+\sigma^2\right) \\ &= \underbrace{\log_2\left(\frac{\alpha_0}{d_h^2+(r_z-w_m^z)^2}\sum_{n\in N_m} p_{m,n}\left(\mathbf{g'}_m^T\mathbf{\Theta}_m\mathbf{g}_{m,n}\right)^2+\sigma^2\right)}_{\gamma'_{m,n}} \\ &\quad \underbrace{-\log_2\left(\frac{\alpha_0}{d_h^2+(r_z-w_m^z)^2}\sum_{n'\in N_{m,n}} p_{m,n'}\left(\mathbf{g'}_m^T\mathbf{\Theta}_m\mathbf{g}_{m,n}\right)^2+\sigma^2\right)}_{\gamma''_{m,n}}, \end{aligned} \tag{24}$$

where

$$d_m^2 = \left(r_x - w_m^x\right)^2 + \left(r_y - w_m^y\right)^2, \tag{25}$$

$$\mathbf{g}_m^T = \mathbf{g'}_m^T\left(\frac{\alpha_0}{d_h^2+\left(r_z-w_m^z\right)^2}\right), and \tag{26}$$

$$\mathbf{g'}_m = \sqrt{\frac{R_m}{R_m+1}}\mathbf{g}_m^{LoS} + \sqrt{\frac{1}{R_m+1}}\mathbf{g}_m^{NLoS}. \tag{27}$$

According to the convex optimization theory, the boundary of $\gamma'_{m,n}$ could be derived with it's first order Taylor expansion w.r.t. $\left(r_z - w_m^z\right)^2$, since the former is convex w.r.t. the latter.

$$\boldsymbol{\varepsilon} = \boldsymbol{\iota}_0 \left(\frac{2 \sum\limits_{n \in N_m} p_{m,n} \left| \mathbf{g}_m^T \boldsymbol{\Theta}_m \mathbf{g}_{m,n} \right| \mathbf{g}_m \mathbf{g}_{m,n}^T}{\ln 2 \sum\limits_{n \in N_m} p_{m,n} (\mathbf{g}_m^T \boldsymbol{\Theta}_m \mathbf{g}_{m,n})^2 + \sigma^2} - \frac{2 \sum\limits_{n' \in N_{m,n}} p_{m,n'} \left| \mathbf{g}_m^T \boldsymbol{\Theta}_m \mathbf{g}_{m,n} \right| \mathbf{g}_m \mathbf{g}_{m,n}^T}{\ln 2 \sum\limits_{n' \in N_{m,n}} p_{m,n'} (\mathbf{g}_m^T \boldsymbol{\Theta}_m \mathbf{g}_{m,n})^2 + \sigma^2} \right) \tag{35}$$

The AoA in $\mathbf{g'_m}$ uses the value in the last iteration to make it easier to solve. Then, $\gamma'_{m,n}$ can be replaced as follows,

$$\begin{aligned} {\gamma'}_{m,n} \geq & \log_2 \left(\frac{\alpha_0}{d_h^2 + (r_z^t - w_m^z)^2} \sum_{n \in N_m} p_{m,n} \left(\mathbf{g'}_m^T \boldsymbol{\Theta}_m \mathbf{g}_{m,n} \right)^2 + \sigma^2 \right) \\ & - \frac{\left((r_z - w_m^z)^2 - \left(r_z^t - w_m^z \right)^2 \right)}{\ln 2 \left(d_h^2 + (r_z^t - w_m^z)^2 \right)^2} \\ & \left(\frac{\alpha_0 \sum\limits_{n \in N_m} p_{m,n} \left(\mathbf{g'}_m^T \boldsymbol{\Theta}_m \mathbf{g}_{m,n} \right)^2}{\frac{\alpha_0}{d_h^2 + (r_z^t - w_m^z)^2} \sum\limits_{n \in N_m} p_{m,n} \left(\mathbf{g'}_m^T \boldsymbol{\Theta}_m \mathbf{g}_{m,n} \right)^2 + \sigma^2} \right) = {\gamma'}_{m,n}^{new}. \end{aligned} \tag{28}$$

where r_z^t denotes the hovering altitude of t-th iteration. Next we introduce an auxiliary variable matrix $\boldsymbol{\mu}$ containing variables μ_m, and let

$$(r_z - w_m^z)^2 \geq \mu_m, \forall m. \tag{29}$$

Based on this transformation, ${\gamma''}_{m,n}$ could be rewritten as

$$\begin{aligned} {\gamma''}_{m,n} \leq & {\gamma''}_{m,n}^{new} \\ = & \log_2 \left(\frac{\alpha_0}{d_h^2 + \mu_m} \sum_{n' \in N_{m,n}} p_{m,n'} \left(\mathbf{g'}_m^T \boldsymbol{\Theta}_m \mathbf{g}_{m,n} \right)^2 + \sigma^2 \right). \end{aligned} \tag{30}$$

Thus, problem (23) can be transformed to

$$\begin{aligned} \max_{r_z, \boldsymbol{\mu}_m} & \sum_{m=1}^{M} \sum_{n=1}^{N} \left({\gamma'}_{m,n}^{new} - {\gamma''}_{m,n}^{new} \right) \\ s.t. \quad & C4, (29). \end{aligned} \tag{31}$$

Note that constraint (29) appears to be concave w.r.t. r_z, thus it is transformed by it's Taylor expansion. And, we can have

$$\mu_m \leq \left(r_z^t - w_m^z \right)^2 + 2 \left(r_z^t - w_m^z \right) \left(r_z - r_z^t \right), \forall m. \tag{32}$$

The hovering altitude optimization problem is finally denoted by the following convex form:

$$\begin{aligned} \max_{r_z, \boldsymbol{\mu}_m} & \sum_{m=1}^{M} \sum_{n=1}^{N} \left({\gamma'}_{m,n}^{new} - {\gamma''}_{m,n}^{new} \right) \\ s.t. \quad & C4, (32). \end{aligned} \tag{33}$$

The following algorithm 2 gives the complete solution flow. Note that adding an iterative loop to the solution process can improve the quality of the final results.

Algorithm 2 SCA based scheme for hovering altitude optimization

1: Initialize the IRS association matrix $\mathbf{v}_{m,n}$ and IRS reflecting coefficient matrix $\boldsymbol{\Theta}_\mathbf{m}$.
2: Initialize a hovering altitude solution r_z^o, the number of iteration $t = 0$, and tolerance ξ.
3: **repeat**
4: Get the hovering altitude solution r_z by solving
$$\begin{aligned} \max_{r_z, \boldsymbol{\mu}_m} & \sum_{m=1}^{M} \sum_{n=1}^{N} \left({\gamma'}_{m,n}^{new} - {\gamma''}_{m,n}^{new} \right) \\ s.t. \quad & C4, (32). \end{aligned}$$
5: $t = t + 1$.
6: $r_z^t = r_z$.
7: **until** $\left| r_z^t - r_z^{t-1} \right| \leq \xi$.

C. Phase Shift Design

After solving the above two problems, the phase shift design problem of multi-IRS is eventually represented by

$$\begin{aligned} \max_{\boldsymbol{\Theta}_m} & \sum_{m=1}^{M} \sum_{n=1}^{N} \gamma_{m,n} \\ s.t. \quad & C5. \end{aligned} \tag{34}$$

Considering the complexity of multiple reflection coefficient matrices, a gradient approximation based univariate optimization (GAUO) solution [47] is utilized in this sub-section to handle the above multivariate optimization problem. This solution consists of two steps to achieve the transformation of it.

Step 1: Let $\gamma_{m,n}(\boldsymbol{\theta}_m)$ denote the sum rate of user n served by IRS m w.r.t. the reflection coefficient matrix $\boldsymbol{\theta}_m$, where $\boldsymbol{\theta}_m = [\theta_{m,1}, \theta_{m,2}, \cdots, \theta_{m,k}, \cdots, \theta_{m,K}]$. Since $\gamma_{m,n}(\boldsymbol{\theta}_m)$ is relatively complicated w.r.t. $\boldsymbol{\theta}_m$, we can approximate the gradient of it via matrix derivation and denote it by (35), where

$$\boldsymbol{\iota}_0 = \left[\underbrace{1, 1, \cdots, 1, 1}_{K} \right]^T \tag{36}$$

denotes the auxiliary vector to satisfy the matrix dimension requirement of δ. Based on the approximated gradient, we can have an improved initial scheme with the metric of the objective through solving

$$\delta = \arg\max_{\delta} \sum_{m=1}^{M} \sum_{n=1}^{N} \gamma_{m,n} \left(\boldsymbol{\theta}_m^0 + \boldsymbol{\varepsilon} \delta \right), \tag{37}$$

where δ denotes the step coefficient, $\boldsymbol{\theta}_m^0$ denotes the initial scheme, and $\left(\boldsymbol{\theta}_m^0 + \varepsilon \delta \right)$ denotes the improved initial scheme. This scheme is a typical univariate problem and can be solved by Fibonacci section.

Step 2: Let $\mathbf{\Delta}_k$ denote k-th column of matrix $\mathbf{\Delta}$, where

$$\mathbf{\Delta} = diag\left(\underbrace{1, 1, \cdots, 1, 1}_{K}\right). \tag{38}$$

The univariate problem for optimizing the k-th reflection element coefficient of IRS m can be denoted by

$$\zeta_{m,k} = \arg\max_{\zeta_{m,k}} \sum_{m=1}^{M} \sum_{n=1}^{N} \gamma_{m,n} \left(\boldsymbol{\theta}_m^j + \mathbf{\Delta}_k \zeta_{m,k}\right). \tag{39}$$

$\zeta_{m,k}$ is the factor coefficient of k-th reflection element of IRS m, and $\boldsymbol{\theta}_m^j$ denotes the results of j-th iteration.

Algorithm 3 GAUO solution for phase shift design

1: Initialize the IRS association matrix $\mathbf{\Theta_m}$ and hovering altitude r_z of UAV.
2: Initialize the reflection coefficient matrix $\boldsymbol{\theta}_m$, $\mathbf{\Delta}$, σ, and $j = 1$.
3: **Step 1**
4: Get improved initial scheme by solving problem (37).
5: $\boldsymbol{\theta}_m^1 = \boldsymbol{\theta}_m^0 + \varepsilon\delta$.
6: **Step 2**
7: **for** $m = 1$ to M **do**
8: **repeat**
9: **for** $k = 1$ to K **do**
10: Get $\zeta_{m,k}$ for given $\boldsymbol{\theta}_m^j$ by solving (39).
11: $\boldsymbol{\theta}_m^j = \boldsymbol{\theta}_m^j + \mathbf{\Delta}_k \zeta_{m,k}$.
12: **end for**
13: $j = j + 1$.
14: **until** $\left|\boldsymbol{\theta}_m^j - \boldsymbol{\theta}_m^{j-1}\right| \leq \sigma$.
15: **end for**

D. Overall Design and Analysis

A three-stage based joint optimization scheme can be developed in algorithm 4 to enhance the quality of overall solutions while improving some complexity. In particular, when M equals to 1, the algorithm evolves into a two-stage joint optimization process. According to the complexity of interior point method, the mathematical complexity in algorithm 1 is calculated by $X_1 M^{3.5}$, where X_1 denotes the number of iteration. And the complexity of algorithm 2 is $X_2 \log\left(\frac{1}{\xi}\right)$, where X_2 is the number of iteration in algorithm 2. The complexity of algorithm 3 can be denoted by MX_3KX_4, where X_3 denotes the number of outer iteration, and X_4 denotes the process of Fibonacci section in step 10. Eventually, the complexity of the proposed joint process is ν

$$\mathcal{O}\left(X\left(\underbrace{X_1 M^{3.5}}_{Stage\ 1} + \underbrace{X_2 \log\left(1/\xi\right)}_{Stage\ 2} + \underbrace{MX_3KX_4}_{Stage\ 3}\right)\right), \tag{40}$$

where X denotes the number of iteration in the outer loop.

Algorithm 4 Three stage based joint optimization process

1: Initialize the IRS association matrix $\mathbf{\Theta^0}$ and hovering altitude r_z^0 of UAV.
2: Initialize $\tau = 0$ and tolerance η.
3: **repeat**
4: $\tau = \tau + 1$.
5: Optimize and get $\mathbf{v}_{m,n}^{\tau}$ by algorithm 1 based on the known $r_z^{\tau-1}$ and $\mathbf{\Theta}^{\tau-\mathbf{1}}$.
6: Optimize and get r_z^{τ} by algorithm 2 based on the known $\mathbf{v}_{m,n}^{\tau}$ and $\mathbf{\Theta}^{\tau-\mathbf{1}}$.
7: Optimize and get $\mathbf{\Theta}^{\tau}$ by algorithm 3 based on the known r_z^{τ} and $\mathbf{v}_{m,n}^{\tau}$.
8: Update the objective f_{obj}^{τ} based on $\mathbf{v}_{m,n}^{\tau}$, r_z^{τ}, and $\mathbf{\Theta}^{\tau}$.
9: **until** $\left|f_{obj}^{\tau} - f_{obj}^{\tau-1}\right| \leq \eta$.

IV. Numerical Results

To demonstrate and verify the rationality of designed scheme in this work, we list some main simulation results in this section. The noise is -174 dBm/Hz [48]. The initial location of UAV is $[0, 0, r_z]^T$, where r_z is 120, 150, or 180 in different scenarios. The number of IRS is set to be 2. The locations of IRSs are $[100, 100, 55]^T$ and $[80, 80, 65]^T$. 10 users are randomly distributed within a reasonable range to receive signals from IRSs, and the maximum number ϑ of users in an IRS is 6. α_0 is set to be 10^{-3}, $R_m = 1$, $R_{m,n} = 1$, and $\frac{d}{w} = 0.5$.The initial association scheme $\mathbf{v}_{m,n}^0 = \{\varpi_{m,n} = 1, \forall m, n\}$. The transmit power of each user is fixed on 0.01 Watt, and each IRS uses a subchannel with the bandwidth 10^6 Hz.

Fig. 3 gives the convergence performance in proposed solution. In Fig. 3(a), there are total 1 IRS, and the IRS is set to associate all users. The two-stage process consists of the hovering altitude of UAV and IRS reflecting coefficient matrix. Fig. 3(b) and Fig. 3(c) depict the convergence of the scheme with 2 IRSs, while the IRS association matrix stays unchanged in Fig. 3(b), and Fig. 3(c) shows the convergence of algorithm 4, as well as the small gap between the proposed algorithm and the optimal scheme obtained by exhaustive search approach. From these three figures, results indicate that the proposed algorithm could converge with a lower number of iteration.

The network deployment is shown in Fig. 4, where the optimized location of UAV is $[0, 0, 64.7255]$ in Fig. 4(a) and $[0, 0, 61.3625]$ in Fig. 4(b), represented by a square. The locations of multi-IRSs are $[80, 80, 65]$, $[100, 100, 56]$, and $[120, 120, 50]$. Fig. 4 also shows the IRS-user association results optimized by proposed interference expansion based algorithm 1, and we can see in Fig. 4(a) that IRS 1 is associated with 4 users, while IRS 2 is associated with the remaining six users. The IRS association coefficient results obtained by algorithm 1 are still binary variables, so the method of rounding is not used to restore the binary variable even after relaxation. When the number of IRS increases, some users will be associated with a more suitable IRS limited to the maximum number associated with one IRS or the network performance, and the altitude of the UAV will change accordingly. In the scenarios, it is assumed that there is an

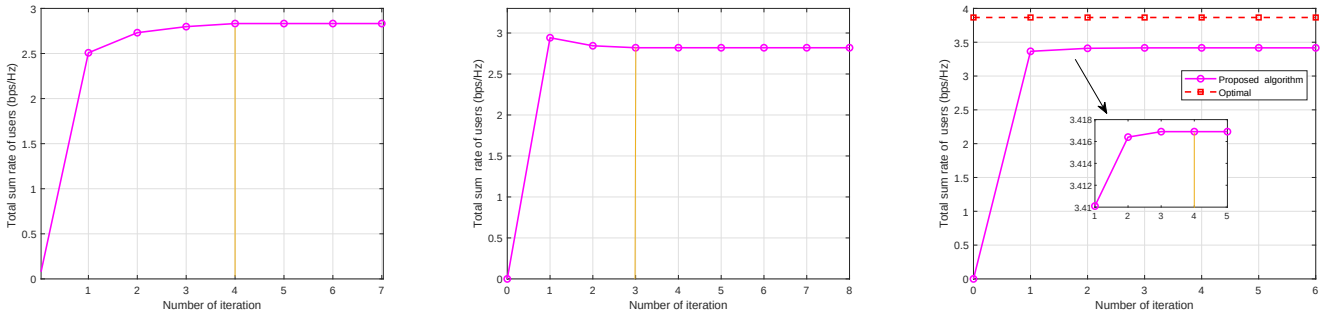

(a) M=1, two-stage process (b) M=2, two-stage process (c) M=2, three-stage process

Fig. 3. The convergence comparison.

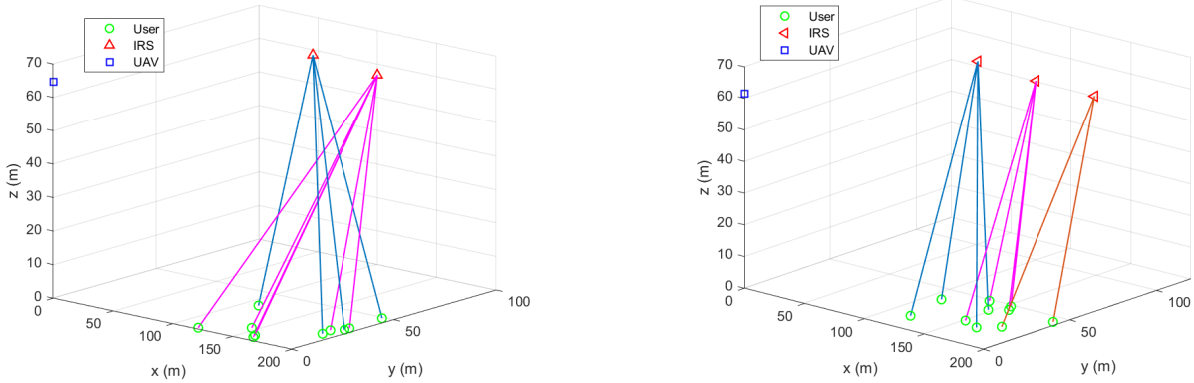

(a) M=2 (b) M=3

Fig. 4. The network deployment and IRS-user association results.

obstacle that hinders communication between users and the UAV, so there is no direct link between these two. Based on this assuming, the locations of users are relatively far from this UAV, and IRSs are deployed at a high position between users and UAV to facilitate communication. Note that it is also assumed that the reflected signal of IRSs can be perfectly passed to users, so the user does not have the case of detachment of the IRS reflection area.

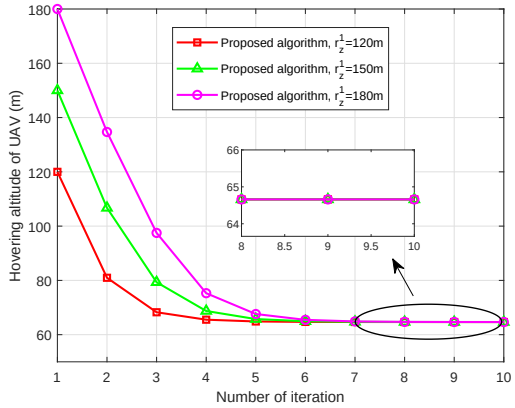

Fig. 5. The optimized hovering altitude of UAV.

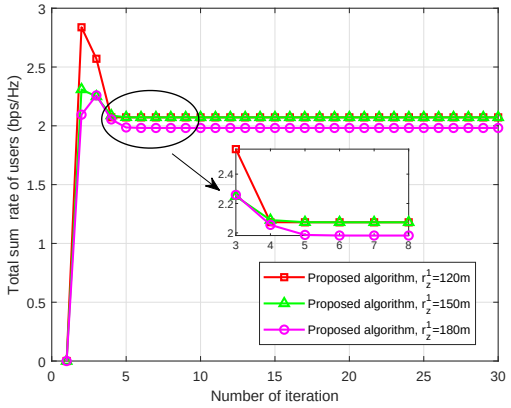

Fig. 6. The sum rate of networks under different initial altitude.

Fig. 5 shows the hovering altitude changes of the UAV after optimization using the proposed algorithm 2 at different initial hovering altitudes. It can be seen that three curves converge to the optimal solution with 5 to 7 iterations. The corresponding network sum rate changes are shown in Fig. 6. The final sum rate does not converge to the same value because the small-scale fading is different for different initial hovering altitude.

The performance of the solved multi-IRS design is dis-

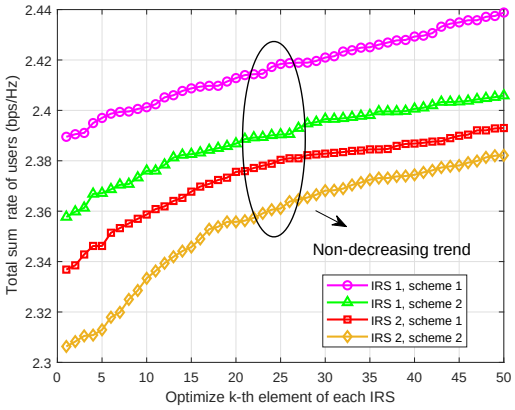

Fig. 7. The sum rate versus the optimization of k-th reflecting element in multi-IRS networks.

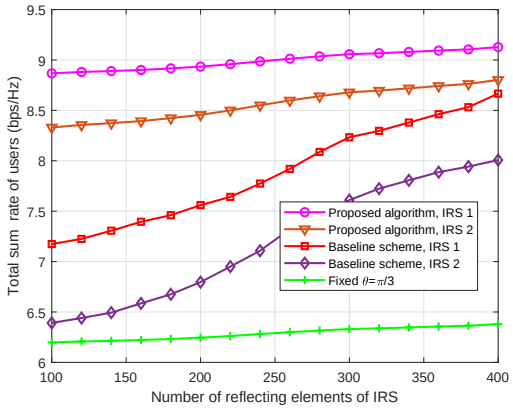

Fig. 8. The sum rate versus the number of reflection elements in multi-IRS networks.

played in Fig. 7. The abscissa indicates the number of elements which are now optimized. The different schemes in the figure represent different initial reflection coefficient results. It can be seen that the entire optimization result is a non-decreasing process, because the proposed scheme is a univariate optimization problem. As the optimization elements increase, the value of the objective function will definitely be equal or higher. Very few values of two adjacent points are the same because the optimization effect of the second point is the same as the initial result of this point, and the corresponding $\zeta_{m,k}$ is equal to 0, so it will not change. There is a gap between different schemes, even if the gap is not large, which means that the proposed algorithm has lost the optimality to a certain extent. However, this can be improved by adding a loop to the outermost layer of the phase shift optimization algorithm.

The results variation of sum rate with different amount of reflecting elements are displayed in Fig. 8. Baseline scheme in this figure represents the existing simplified univariate search method. From the analysis of results, the sum rate of these two IRSs under different schemes shows incremental changes following the replenishment of reflecting elements in multi-IRS, because the increase in the number of elements also produces higher channel gain. At the same time, the proposed optimization algorithm performs better than the baseline scheme because the initial value of the proposed algorithm is better. The fixed scheme of IRS 1 is put at the end for comparison. Note that the obtained sum rate at this time tends to be obviously higher than the results in previous figures as the number of elements in IRS in the simulation here is larger than before.

We also set up different number of served users to test results obtained by designed multi-IRS scheme in Fig. 9 and Fig. 10. When $m = 1$, the only IRS still has to perform association optimization, instead of directly associating all users. The numerical size of ϑ exceeds all users when there are 4 or 5 users, so the optimized association results show that the IRS is associated with all users actually. Intuitively, the relationship between the number of users in the multi-IRS network and optimized sum rate is a linearly increasing process in Fig. 9. This is because the number of users

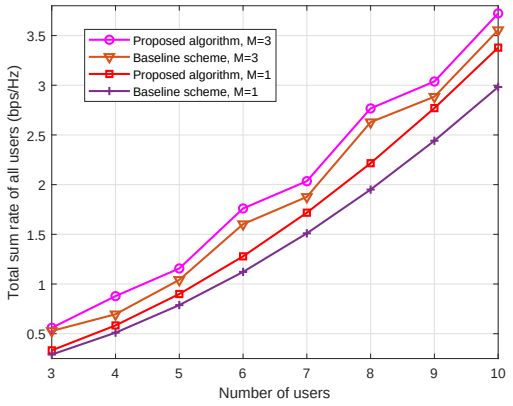

Fig. 9. The sum rate versus the number of users with different number of IRS.

served by network also increases, so it can choose users with better gains to serve when we add more users to the simulation scenario. The sum rate in proposed scheme is slightly higher than that in the baseline scheme, and the accumulated advantage still exists when the number of IRS also increases. The proposed algorithm was compared with the scheme without any optimization in Fig. 10, where we can find the performance improvement by the proposed algorithm.

V. Conclusion

In this paper, we designed a hovering UAV based multi-IRS NOMA network to achieve communication across ground obstacles. A three-stage joint optimization process involving IRS association, hovering altitude, and phase shift design in multi-IRS was designed to maximize the network sum rate. Particularly, a mathematical interference expansion scheme was proposed to make the convex optimization transformation of the IRS association problem by decoupling the user association and SIC decoding of NOMA. The hovering altitude optimization problem of UAV was converted into the convex to solve by means of logarithmic operation, relaxation, and auxiliary variables. Finally, we used a GA method based univariate search approach to optimize the reflecting coeffi-

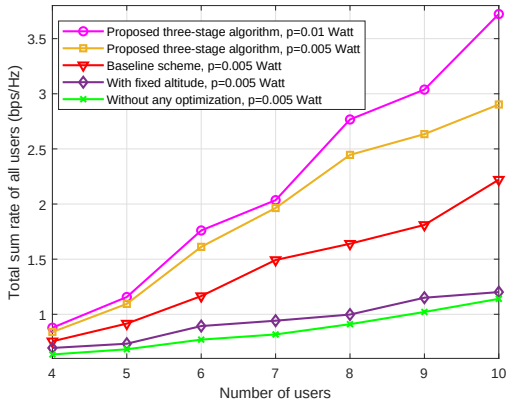

Fig. 10. The sum rate versus the number of users with different power.

cient problem for multiple IRSs. The simulation results at the end showed that our proposed optimization scheme can outperform the baseline scheme. This work also presented and analyzed how the performance results changed with some network parameters to fully explain our design.

REFERENCES

[1] H. Hashida, Y. Kawamoto, and N. Kato, "Intelligent reflecting surface placement optimization in air-ground communication networks toward 6G," *IEEE Wireless Commun.*, vol. 27, no. 6, pp. 146-151, Dec. 2020.

[2] V. Jamali, H. Ajam, M. Najafi, B. Schmauss, R. Schober, and H. V. Poor, "Intelligent reflecting surface assisted free-space optical communications," *IEEE Commun. Mag.*, vol. 59, no. 10, pp. 57-63, Oct. 2021.

[3] C. You, Z. Kang, Y. Zeng, and R. Zhang,"Enabling smart reflection in integrated air-ground wireless network: IRS meets UAV," *IEEE Wireless Commun.*, vol. 28, no. 6, pp. 138-144, Dec. 2021.

[4] A. S. d. Sena et al., "What role do intelligent reflecting surfaces play in multi-antenna non-orthogonal multiple access?," *IEEE Wireless Commun.*, vol. 27, no. 5, pp. 24-31, Oct. 2020.

[5] X. Yu, V. Jamali, D. Xu, D. W. K. Ng, and R. Schober, "Smart and reconfigurable wireless communications: From IRS modeling to algorithm design," *IEEE Wireless Commun.*, vol. 28, no. 6, pp. 118-125, Dec. 2021.

[6] S. Buzzi, C. DAndrea, A. Zappone, M. Fresia, Y. -P. Zhang, and S. Feng, "RIS configuration, beamformer design, and power control in single-cell and multi-cell wireless networks," *IEEE Trans. Cognit. Commun. Networking*, vol. 7, no. 2, pp. 398-411, Jun. 2021.

[7] Y. Li, H. Zhang, and K. Long, "Joint resource, trajectory, and artificial noise optimization in secure driven 3-D UAVs with NOMA and imperfect CSI," *IEEE J. Sel. Areas Commun.*, vol. 39, no. 11, pp. 3363-3377, Nov. 2021.

[8] Q. Wu, X. Zhou, and R. Schober, "IRS-assisted wireless powered NOMA: do we really need different phase shifts in DL and UL?," *IEEE Wireless Commun. Lett.*, vol. 10, no. 7, pp. 1493-1497, Jul. 2021.

[9] B. Zheng, C. You, and R. Zhang, "Double-IRS assisted multi-user MIMO: Cooperative passive beamforming design," *IEEE Trans. Wireless Commun.*, vol. 20, no. 7, pp. 4513-4526, Jul. 2021.

[10] E. Shtaiwi, H. Zhang, S. Vishwanath, M. Youssef, A. Abdelhadi, and Z. Han, "Channel estimation approach for RIS assisted MIMO systems," *IEEE Trans. Cognit. Commun. Networking*, vol. 7, no. 2, pp. 452-465, Jun. 2021.

[11] H. Ur Rehman, F. Bellili, A. Mezghani and E. Hossain, "Joint active and passive beamforming design for IRS-assisted multi-user MIMO systems: A VAMP-based approach," *IEEE Trans. Commun.*, vol. 69, no. 10, pp. 6734-6749, Oct. 2021.

[12] I. Yildirim, A. Uyrus, and E. Basar, "Modeling and analysis of reconfigurable intelligent surfaces for indoor and outdoor applications in future wireless networks," *IEEE Trans. Commun.*, vol. 69, no. 2, pp. 1290-1301, Feb. 2021.

[13] H. Albinsaid, K. Singh, A. Bansal, S. Biswas, C. -P. Li, and Z. J. Haas, "Multiple antenna selection and successive signal detection for SM-based IRS-aided communication," *IEEE Signal Process. Lett.*, vol. 28, pp. 813-817, 2021.

[14] F. Fang, Y. Xu, Q. -V. Pham, and Z. Ding, "Energy-efficient design of IRS-NOMA networks," *IEEE Trans. Veh. Technol.*, vol. 69, no. 11, pp. 14088-14092, Nov. 2020.

[15] S. Hu, Z. Wei, Y. Cai, C. Liu, D. W. K. Ng, and J. Yuan, "Robust and secure sum-rate maximization for multiuser MISO downlink systems with self-sustainable IRS," *IEEE Trans. Commun.*, vol. 69, no. 10, pp. 7032-7049, Oct. 2021.

[16] E. Basar, "Reconfigurable intelligent surface-based index modulation: A new beyond MIMO paradigm for 6g," *IEEE Trans. Commun.*, vol. 68, no. 5, pp. 3187-3196, May 2020.

[17] S. Dhok, P. Raut, P. K. Sharma, K. Singh, and C. P. Li, "Non-linear energy harvesting in RIS-assisted URLLC networks for industry automation," *IEEE Trans. Commun.*, vol. 69, no. 11, pp. 7761-7774, Nov. 2021.

[18] T. Shafique, H. Tabassum, and E. Hossain, "Optimization of wireless relaying with flexible UAV-borne reflecting surfaces," *IEEE Trans. Commun.*, vol. 69, no. 1, pp. 309-325, Jan. 2021.

[19] G. Iacovelli, A. Coluccia, and L. A. Grieco, "Channel gain lower bound for IRS-assisted UAV-aided communications," *IEEE Commun. Lett.*, vol. 25, no. 12, pp. 3805-3809, Dec. 2021.

[20] X. Liu, H. Zhang, K. Long, M. Zhou, Y. Li, and H. Vincent Poor, "Proximal policy optimization-based transmit beamforming and phase-shift design in an IRS-aided ISAC system for the THz Band," *IEEE J. Sel. Areas Commun.*, early access.

[21] H. Zhang, B. Di, Z. Han, H. V. Poor, and L. Song, "Reconfigurable intelligent surface assisted multi-user communications: How many reflective elements do we need?," *IEEE Wireless Commun. Lett.*, vol. 10, no. 5, pp. 1098-1102, May 2021.

[22] M. Elhattab, M. A. Arfaoui, C. Assi, and A. Ghrayeb, "RIS-assisted joint transmission in a two-cell downlink NOMA cellular system," *IEEE J. Sel. Areas Commun.*, vol. 40, no. 4, pp. 1270-1286, Apr. 2022.

[23] A. Papazafeiropoulos, P. Kourtessis, S. Chatzinotas, and J. M. Senior, "Coverage probability of double-IRS assisted communication systems," *IEEE Wireless Commun. Lett.*, vol. 11, no. 1, pp. 96-100, Jan. 2022.

[24] T. N. Do, G. Kaddoum, T. L. Nguyen, D. B. da Costa, and Z. J. Haas, "Multi-RIS-aided wireless systems: Statistical characterization and performance analysis," *IEEE Trans. Commun.*, vol. 69, no. 12, pp. 8641-8658, Dec. 2021.

[25] A. Bansal, K. Singh, B. Clerckx, C. -P. Li, and M. -S. Alouini, "Rate-splitting multiple access for intelligent reflecting surface aided multi-user communications," *IEEE Trans. Veh. Technol.*, vol. 70, no. 9, pp. 9217-9229, Sept. 2021.

[26] Z. Ding and H. Vincent Poor, "A simple design of IRS-NOMA transmission," *IEEE Commun. Lett.*, vol. 24, no. 5, pp. 1119-1123, May 2020.

[27] A. H. Abdollahi Bafghi, V. Jamali, M. Nasiri-Kenari, and R. Schober, "Degrees of freedom of the k-user interference channel assisted by active and passiveIRSs," *IEEE Trans. Commun.*, early access.

[28] M. He, W. Xu, H. Shen, G. Xie, C. Zhao, and M. Di Renzo, "Cooperative multi-RIS communications for wideband mmwave MISO-OFDM systems," *IEEE Wireless Commun. Lett.*, vol. 10, no. 11, pp. 2360-2364, Nov. 2021.

[29] M. Najafi, V. Jamali, R. Schober, and H. V. Poor, "Physics-based modeling and scalable optimization of large intelligent reflecting surfaces," *IEEE Trans. Commun.*, vol. 69, no. 4, pp. 2673-2691, Apr. 2021.

[30] X. Yu, D. Xu, Y. Sun, D. W. K. Ng, and R. Schober,"Robust and secure wireless communications via intelligent reflecting surfaces," *IEEE J. Sel. Areas Commun.*, vol. 38, no. 11, pp. 2637-2652, Nov. 2020.

[31] J. Choi, G. Kwon, and H. Park,"Multiple intelligent reflecting surfaces for capacity maximization in LoS MIMO systems," *IEEE Wireless Commun. Lett.*, vol. 10, no. 8, pp. 1727-1731, Aug. 2021.

[32] A. Abrardo, D. Dardari, and M. Di Renzo, "Intelligent reflecting surfaces: Sum-rate optimization based on statistical position information," *IEEE Trans. Commun.*, vol. 69, no. 10, pp. 7121-7136, Oct. 2021.

[33] E. Bjrnson and L. Sanguinetti, "Power scaling laws and near-field behaviors of massive MIMO and intelligent reflecting surfaces," *IEEE Open J. Commun. Soc.*, vol. 1, pp. 1306-1324, Sept. 2020.

[34] C. Pan et al., "Multicell MIMO communications relying on intelligent reflecting surfaces," *IEEE Trans. Wireless Commun.*, vol. 19, no. 8, pp. 5218-5233, Aug. 2020.

[35] H. Zhang, J. Zhang, and K. Long, "Energy efficiency optimization for NOMA UAV network with imperfect CSI," *IEEE J. Sel. Areas Commun.*, vol. 38, no. 12, pp. 2798-2809, Dec. 2020.

[36] M. Al-Jarrah, A. Al-Dweik, E. Alsusa, Y. Iraqi, and M. S. Alouini, "On the performance of IRS-assisted multi-layer UAV communications with imperfect phase compensation," *IEEE Trans. Commun.*, vol. 69, no. 12, pp. 8551-8568, Dec. 2021.
[37] A. Mahmoud, S. Muhaidat, P. C. Sofotasios, I. Abualhaol, O. A. Dobre, and H. Yanikomeroglu, "Intelligent reflecting surfaces assisted UAV communications for IoT networks: Performance analysis," *IEEE Trans. Green Commun. Networking*, vol. 5, no. 3, pp. 1029-1040, Sept. 2021.
[38] M. Samir, M. Elhattab, C. Assi, S. Sharafeddine, and A. Ghrayeb, "Optimizing age of information through aerial reconfigurable intelligent surfaces: A deep reinforcement learning approach," *IEEE Trans. Veh. Technol.*, vol. 70, no. 4, pp. 3978-3983, Apr. 2021.
[39] S. Li, B. Duo, X. Yuan, Y. Liang, and M. Di Renzo, "Reconfigurable intelligent surface assisted UAV communication: Joint trajectory design and passive beamforming," *IEEE Wireless Commun. Lett.*, vol. 9, no. 5, pp. 716-720, May 2020.
[40] X. Zhang, H. Zhang, W. Du, K. Long, and A. Nallanathan, "IRS empowered UAV wireless communication with resource allocation, reflecting design and trajectory optimization," *IEEE Trans. Wireless Commun.*, early access.
[41] M. Hua, L. Yang, Q. Wu, C. Pan, C. Li, and A. L. Swindlehurst, "UAV-assisted intelligent reflecting surface symbiotic radio system," *IEEE Trans. Wireless Commun.*, vol. 20, no. 9, pp. 5769-5785, Sept. 2021.
[42] Z. Wei, Y. Cai, Z. Sun, D. W. K. Ng, et al., "Sum-rate maximization for IRS-assisted UAV OFDMA communication systems," *IEEE Trans. Wireless Commun.*, vol. 20, no. 4, pp. 2530-2550, Apr. 2021.
[43] S. Fang, G. Chen, and Y. Li, "Joint optimization for secure intelligent reflecting surface assisted UAV networks," *IEEE Wireless Commun. Lett.*, vol. 10, no. 2, pp. 276-280, Feb. 2021.
[44] N. Agrawal, A. Bansal, K. Singh, C. P. Li, and S. Mumtaz, "Finite block length analysis of RIS-assisted UAV-based multiuser IoT communication system with non-linear EH," *IEEE Trans. Wireless Commun.*, early access.
[45] X. Liu, Y. Liu, and Y. Chen, "Machine learning empowered trajectory and passive beamforming design in UAV-RIS wireless networks," *IEEE J. Sel. Areas Commun.*, vol. 39, no. 7, pp. 2042-2055, Jul. 2021.
[46] S. T. Muntaha, S. A. Hassan, H. Jung and M. S. Hossain, "Energy efficiency and hover time optimization in UAV-based HetNets," *IEEE Trans. Intell. Transp. Syst.*, vol. 22, no. 8, pp. 5103-5111, Aug. 2021.
[47] G. Beveridge and R. Schechter, "Optimization: Theory and practice," McGraw-Hill, New York, 1970.
[48] Y. Li, H. Zhang, K. Long, C. Jiang, and M. Guizani,"Joint resource allocation and trajectory optimization with QoS in UAV-based NOMA wireless networks," *IEEE Trans. Wireless Commun.*, vol. 20, no. 10, pp. 6343-6355, Oct. 2021.

Yabo Li is currently pursuing his Ph.D. degree at University of Science and Technology Beijing, China. His research interests include resource allocation with the emphasis on UAV or UAV-assisted wireless networks, and intelligent reflecting surface. He serves as a TPC member for IEEE VTC2022-Fall, and Reviewer for IEEE Transactions on Communications and several journals.

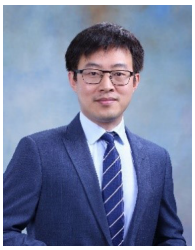

Haijun Zhang (M'13, SM'17) is currently a Full Professor and Associate Dean at University of Science and Technology Beijing, China. He was a Postdoctoral Research Fellow in Department of Electrical and Computer Engineering, the University of British Columbia (UBC), Canada. He serves/served as Track Co-Chair of WCNC 2020, Symposium Chair of Globecom'19, TPC Co-Chair of INFOCOM 2018 Workshop on Integrating Edge Computing, Caching, and Offloading in Next Generation Networks, and General Co-Chair of GameNets'16. He serves as an Editor of IEEE Transactions on Communications, IEEE Transactions on Network Science and Engineering, and IEEE Transactions on Vehicular Technology. He received the IEEE CSIM Technical Committee Best Journal Paper Award in 2018, IEEE ComSoc Young Author Best Paper Award in 2017, and IEEE ComSoc Asia-Pacific Best Young Researcher Award in 2019.

Keping Long (SM'06) received the M.S. and Ph.D. degrees from the University of Electronic Science and Technology of China, Chengdu, in 1995 and 1998, respectively. From September 1998 to August 2000, he was a Postdoctoral Research Fellow at the National Laboratory of Switching Technology and Telecommunication Networks, Beijing University of Posts and Telecommunications (BUPT), China. From September 2000 to June 2001, he was an Associate Professor at BUPT. From July 2001 to November 2002, he was a Research Fellow with the ARC Special Research Centre for Ultra Broadband Information Networks (CUBIN), University of Melbourne, Australia. He is currently a professor and Dean at the School of Computer and Communication Engineering, University of Science and Technology Beijing. He has published more than 200 papers, 20 keynote speeches, and invited talks at international and local conferences. His research interests are optical Internet technology, new generation network technology, wireless information networks, value-added services, and secure technology of networks. Dr. Long had been a TPC or ISC member of COIN 2003/04/05/06/07/08/09/10, IEEE IWCN2010, ICON2004/06, APOC2004/06/08, Co-Chair of the organization Committee for IWCMC2006, TPC Chair of COIN 2005/08, and TPC Co-Chair of COIN 2008/10. He was awarded by the National Science Fund for Distinguished Young Scholars of China in 2007 and selected as the Chang Jiang Scholars Program Professor of China in 2008. He is a member of the Editorial Committees of Sciences in China Series F and China Communications.